Emodin inhibits HDAC6 mediated NLRP3 signaling and relieves chronic inflammatory pain in mice

DING-WEN CHENG[1*], YIWEN XU[2*], TAO CHEN[2*], SHU-QING ZHEN[3], WEI MENG[4], HAI-LI ZHU[4], LING LIU[4], MIN XIE[4] and FANGSHOU ZHEN[3]

[1]School of Pharmacy, Hubei University of Science and Technology; [2]Department of Pharmacy, Xianning Central Hospital, First Affiliated Hospital of Hubei University of Science and Technology; [3]Department of Pharmacy, Matang Hospital of Traditional Chinese Medicine; [4]Hubei Key Laboratory of Diabetes and Angiopathy, School of Basic Medical Sciences, Xianning Medical College, Hubei University of Science and Technology, Xianning, Hubei 437100, P.R. China

Received June 21, 2023; Accepted September 28, 2023

DOI: 10.3892/etm.2023.12332

Abstract. Chronic pain reduces the quality of life and ability to function of individuals suffering from it, making it a common public health problem. Neuroinflammation which is mediated by the Nod-like receptor family pyrin domain-containing 3 (NLRP3) inflammasome activation in the spinal cord participates and modulates chronic pain. A chronic inflammatory pain mouse model was created in the current study by intraplantar injection of complete Freund's adjuvant (CFA) into C57BL/6J left foot of mice. Following CFA injection, the mice had enhanced pain sensitivities, decreased motor function, increased spinal inflammation and activated spinal astrocytes. Emodin (10 mg/kg) was administered intraperitoneally into the mice for 3 days. As a result, there were fewer spontaneous flinches, higher mechanical threshold values and greater latency to fall. Additionally, in the spinal cord, emodin administration reduced leukocyte infiltration level, down-regulated protein level of IL-1β, lowered histone deacetylase (HDAC)6 and NLRP3 inflammasome activity and suppressed astrocytic activation. Emodin also binds to HDAC6 via four electrovalent bonds. In summary, emodin treatment blocked the HDAC6/NLRP3 inflammasome signaling, suppresses spinal inflammation and alleviates chronic inflammatory pain.

Correspondence to: Dr Min Xie, Hubei Key Laboratory of Diabetes and Angiopathy, School of Basic Medical Sciences, Xianning Medical College, Hubei University of Science and Technology, 88 Xianning Road, Xianning, Hubei 437100, P.R. China
E-mail: xiemin2020a@163.com

Dr Fangshou Zhen, Matang Hospital of Traditional Chinese Medicine, 2 Guixiang Road, Xianning, Hubei 437100, P.R. China
E-mail: 195950528@qq.com

*Contributed equally

Key words: emodin, chronic inflammatory pain, Nod-like receptor family pyrin domain-containing 3 inflammasome, histone deacetylase 6

Introduction

Chronic pain often lasts months or years, affecting >20% of adults worldwide and developing into a widespread public health issue. Chronic pain significantly affects the patients' ability to sleep, work and study, which lowers their quality of life and ability to function (1). Spontaneous pain and evoked pain in reaction to non-noxious or noxious stimuli are characteristics of chronic pain (2). Preferred pharmacologic treatments consist of opioids, acetaminophen and nonsteroidal anti-inflammatory drugs. Due to gastrointestinal discomfort along with other side effects of drugs, nearly one-third of patients were unsatisfied with their treatment (3). Thus, developing new analgesic drugs with fewer side effects is essential.

Neuroinflammation in the spinal cord participates in and modulates chronic pain, which is marked by the release of inflammatory mediators and glial cell activation (4,5). During pain processing, tissue injury generates a number of nociceptive stimuli that cause primary afferent fibers. After transmitting to the spinal cord, these nociceptive signals activate astrocytes and nociceptors (6). Activated astrocytes undergo hyperplasia and hypertrophy and release several pro-inflammatory mediators, for instance IL-1β, which is known to mediate pain and sensitize nociceptors directly (7). The Nod-like receptor family pyrin domain-containing 3 (NLRP3) inflammasome is well-characterized for IL-1β maturation (8). NLRP3 inflammasome assembly allows the cleavage of caspase-1 and in turn leads IL-1β secretion and NF-κB activation (9,10). The pathophysiology of chronic pain is influenced by the dysregulation of NLRP3 inflammasome (11). IL-1β, apoptosis-associated speck-like protein (ASC) and caspase-1 are among the NLRP3 inflammasome components whose spinal expression is greatly elevated in the complete Freund's adjuvant (CFA)-induced inflammatory pain model (12). MCC950 (a specific inhibitor of NLRP3) or *Nlrp3* gene knockout therapy reduces inflammatory pain in mice (13). Hence, targeting NLRP3 inflammation activation is a potential therapy for chronic pain.

Traditional Chinese medicine uses emodin (1,3,8-trihydroxy-6-methylanthraquinone), which is a natural anthraquinone derivative and found in *Rheum palmatum* and a number of other plants. Emodin possesses a number of benefits, including those against cancer, inflammation, viruses and bacteria (14). In several pain models, such as capsaicin, acetic acid, carrageenan and formalin-induced pain, emodin decreases nociceptive and inflammatory responses (15). Emodin treatment alleviates hyperalgesia by decreasing the P2X (2/3) expression in chronic constriction injury neuropathic pain model rats (16). Consequently, targeting HDAC6 is favorable for managing chronic pain as well as neuroinflammation.

In order to establish a chronic inflammatory pain model an intraplantar injection of CFA in the left foot of C57BL/6J mice was performed. For three successive days intraperitoneal injections of emodin were performed. The related protein expression levels, changes in behaviors and spinal inflammation were detected. It was intended to explain how emodin works to reduce chronic pain and provide theoretical and data support for emodin application in chronic pain treatment.

Materials and methods

Animal model and drug administration. Male C57BL/6J mice (6-8 weeks old; 18-20 g; n=30) were bought from the Hubei Province Experimental Animal Centre. Animals were kept under 12 h light/dark environment and unlimited access to food and water. The experiment was approved by the Laboratory Animal Ethics Committee of Hubei University of Science and Technology (approval no 2019-03-021).

Prior to the test, mice were randomly divided into Control, CFA and CFA + emodin groups, 10 mice for each group. There was a 7-day period of acclimation to the surroundings. Then on days 0 and 7, left hind paws of mice received intraplantar subcutaneous injections of 10 μl CFA and the equal amount of saline was administered in mice from control group (17). On days 0, 7 and 14, behavioral assessments were conducted. On days 15-17 following the CFA injection, vehicle and emodin (10 mg/kg) were intraperitoneally injected in CFA and CFA + emodin groups for 3 days. Prior to use, emodin was dissolved in DMSO which diluted with 0.9% NaCl. After 4 h of emodin treatment, the behavioral tests were conducted.

Antibodies and reagents. Anti-NLRP3 (cat. no. DF7438), anti-HDAC6 (cat. no. AF6485), anti-glial fibrillary acidic protein (GFAP, cat. no. BF0345), anti-IL-1β (cat. no. AF5103), anti-β-actin (cat. no. AF7018) and anti-cleaved caspase-1 (cat. no. AF4022) antibodies were purchased from Affinity Biosciences. Anti-caspase-1 (cat. no. A0964), HRP Goat anti-rabbit IgG (H+L; cat. no. AS014) and HRP Goat anti-mouse IgG (H+L; cat. no. AS003) antibodies were acquired from ABclonal Biotech Co., Ltd. H&E staining kit (cat. no. BL735B) was bought from Biosharp Life Sciences. Emodin was purchased from Shanghai Yuanye Biotechnology Co., Ltd. Goat Anti-Rabbit IgG H&L (FITC; cat. no. ab6717) and Goat Anti-Mouse IgG H&L (TRITC; cat. no. ab6786) were from Abcam.

Mechanical threshold test. Mice were housed in a plexiglass container to acclimatize for almost 30 min. Then, von Frey filaments (Stoelting Co.) were applied to stimulate the left hind paw. The filaments were briefly bent by being pushed firmly vertically on the plantar surfaces for 3-5 sec. Paw flinching and brisk withdrawal were regarded as positive responses in this circumstance. The patterns of withdrawal responses were then translated into mechanical threshold values (18).

Spontaneous flinch test. Mice were housed for nearly 30 mins in a plexiglass chamber. Within 5 min, numbers of flinches were counted 3 times individually (19).

Rotarod test. Mice were trained three days at a fixed pace for 10 min before the examinations. In the experiments, the test was initially set at a constant speed at 10 revolutions per min for 10 sec, then at an increasing speed to 20 revolutions per min for 30 sec. The latency to fall was measured to evaluate the balance and motor coordination of the animals (20).

H&E staining. Following the behavior test, mice were given a deep anesthetic dose of 60 mg/kg sodium pentobarbital and transcardially perfused using 4% PFA. After collection and post-fixation using 4% PFA for 12 h at 4˚C, the spinal cords were embedded with paraffin and cutting into 4-μm sections. The sections were treated with xylene, 100, 90 and 70% ethanol and dyed with H&E staining kit. Briefly, paraffin sections were treated with xylene (5 min, twice), 100% ethanol (10 min, twice), 90% ethanol (10 min) and 70% ethanol (10 min) for dewaxing, then stained with hematoxylin solution for 3 min at 25˚C and eosin for 3 min at 25˚C. The slices were treated with 70% ethanol (10 sec), 80% ethanol (10 sec), 90% ethanol (30 sec), 100% ethanol (1 min, twice) and xylene (1 min, twice) to dehydrate the sample and render it transparent, sealed with neutral balsam, images captured under a fluorescence microscope (IX73; Olympus Corporation) and analyzed using ImageJ 1.48v (National Institutes of Health). Inflammatory cell infiltration was categorized as 0 (normal); 1 (meningeal and perivascular lymphocytic infiltration); 2 (1-10 lymphocytes present); 3 (11-100 lymphocytes); and 4 (>100 lymphocytes).

Immunofluorescence. The sections of spinal cord tissue were hydrated and subjected to antigen retrieval using antigen retrieval solution (cat. no. P0083; Beyotime Institute of Biotechnology) for 10 min at 95˚C. The sections were blocked with immunofluorescence blocking solution (cat. no. P0102; Beyotime Institute of Biotechnology) for 1h before incubating with primary antibody at 4˚C overnight and fluorescent secondary antibodies for 1 h at room temperature. The images were captured by a fluorescence microscope and analyzed using ImageJ 1.48v (National Institutes of Health). The primary antibodies were anti-HDAC6, anti-IL-1β, anti-caspsae-1, anti-GFAP and anti-NLRP3, the dilution ratio was 1:100.

Western blotting. Mice were intraperitoneally injected with 150 mg/kg pentobarbital sodium after the behavioral tests. The lumbar spinal cords were homogenized in RIPA lysis buffer containing 1% protease inhibitors (MilliporeSigma) and centrifuged for 20 min (12,000 x g, 4˚C). The supernatant was

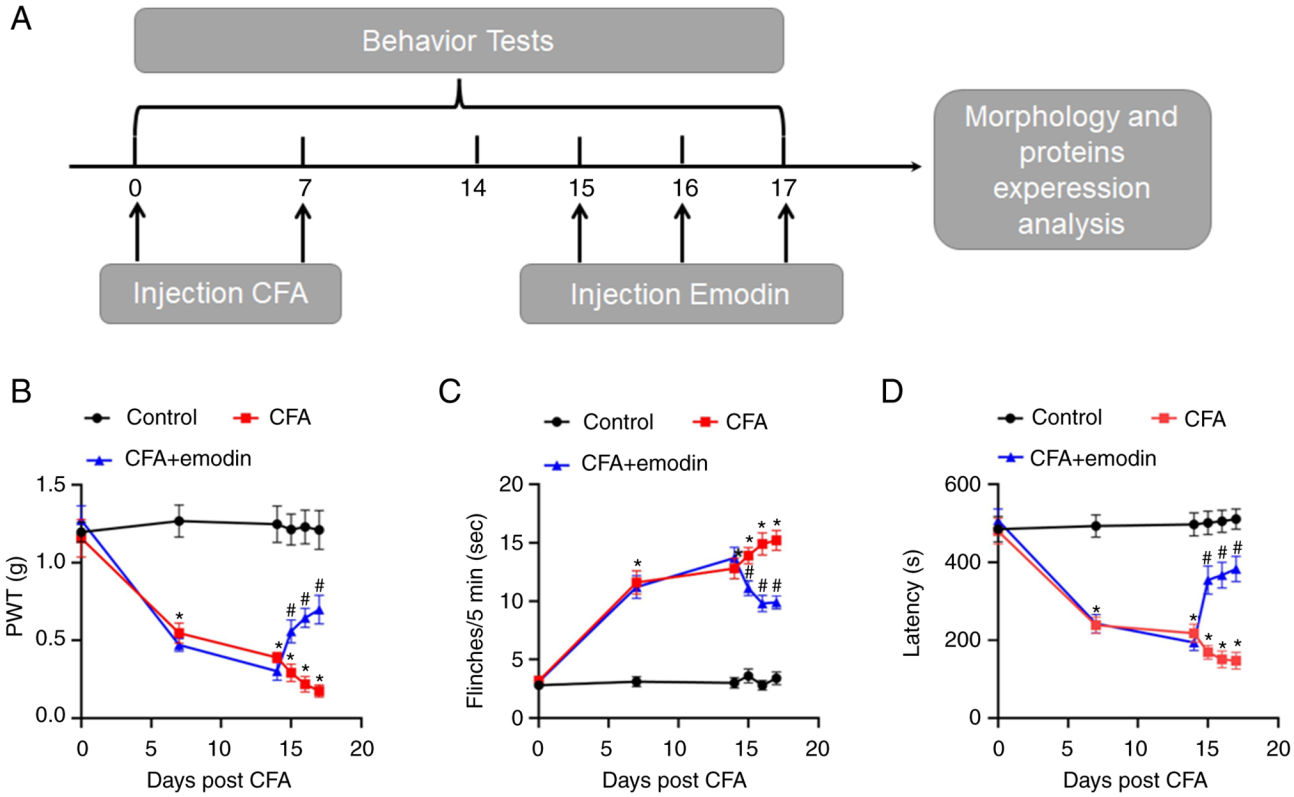

Figure 1. Effect of emodin on pain behaviors. (A) Schematic diagram of the experimental process. Changes of (B) PWT values, (C) numbers of spontaneous flinches and (D) latency to fall in different groups. Data are presented as the mean ± SEM (n=10). *P<0.05 vs. control group; #P<0.05 vs. CFA group. PWT, paw withdrawal threshold; CFA, complete Freund's adjuvant.

quantified using a BCA analysis kit (cat. no. P0012; Beyotime Institute of Biotechnology). Protein mixture samples were loaded at 20 μg/lane and separated using 10-15% SDS-PAGE. The blots were transferred to PVDF membranes. Following a blocking using QuickBlock Blocking Buffer (cat. no. P0220; Beyotime Institute of Biotechnology) at 4˚C for 15 min, the membranes were incubated with primary antibodies overnight at 4˚C and secondary antibodies (1:5,000) for 1 h (room temperature). The bands were visualized using ECL solution (cat. no. P0018M; Beyotime Institute of Biotechnology) and analyzed using ImageJ 1.48v (National Institutes of Health). β-actin was used as a loading control. The following primary antibodies were used: anti-GFAP (1:1,000), anti-IL-1β (1:1,000), anti-cleaved-caspsae-1 (1:1,000), anti-HDAC6 (1:1,000), anti-NLRP3 (1:1,000) and anti-β-actin (1:50,000).

Molecular docking. HDAC6 X-ray crystal structure was acquired through Protein Data Bank (PDB ID, 5B8D; https://www.rcsb.org/structure/5B8D). The structure of emodin was optimized and retrieved from the PubChem compound database (PubChem CID, 3220; https://pubchem.ncbi.nlm.nih.gov/compound/3220). Docking conformation among emodin and HDAC6 was employed by Auto Dock Vina 1.2.0 software (Center for Computational Structural Biology, https://vina.scripps.edu/downloads/). The conformation was seen using PyMOL 2.2.3 (21).

Statistical analysis. All statistical analyses were performed using SPSS 26.0 (IBM Corp.). Data of H&E staining, behaviors, western blotting and immunofluorescence were examined by a one-way ANOVA followed by Tukey's post-hoc test. Data for paw withdrawal threshold (PWT), flinches and latency to fall are expressed as mean ± SEM. Data for histology, morphology and western blotting are expressed as the mean ± SD.

Results

Emodin decreases pain sensitivity in CFA-induced mice. Fig. 1A indicates the experiment process including the behavioral tests. As shown in Fig. 1B, mechanical threshold values in the CFA mice were lowered with the PWT values of day 0, 7 and 14 at 1.15 ± 0.12, 0.55 ± 0.06 and 0.39 ± 0.03, respectively. The number of flinches (Fig. 1C) raised in CFA mice, from 3.20 ± 0.36 (day 0) to 11.60 ± 1.01 (day 7), 12.80 ± 0.89 (day 14), compared with control mice. In contrast to control mice, the latency to fall (Fig. 1D) in CFA mice decreased from 480.03 ± 33.27 (day 0) to 238.53 ± 20.75 (day 7) and 217.90 ± 23.67 (day 14). As suggested by the data, CFA results in motor disability as well as nociceptive hyperalgesia in mice, which indicated that the mouse model of chronic pain had been constructed effectively. The impact of emodin on motor function and pain sensitivity was then evaluated. The values of mechanical threshold in CFA + emodin mice were higher after emodin treatment on days 15-17, which are 0.56 ± 0.07, 0.64 ± 0.06 and 0.70 ± 0.09, respectively (Fig. 1B). There were significantly fewer flinches in the CFA + emodin mice, 11.10 ± 0.62 (day 15), 9.80 ± 0.70 (day 16) and 9.90 ± 0.57 (day 17), respectively (Fig. 1C). The emodin

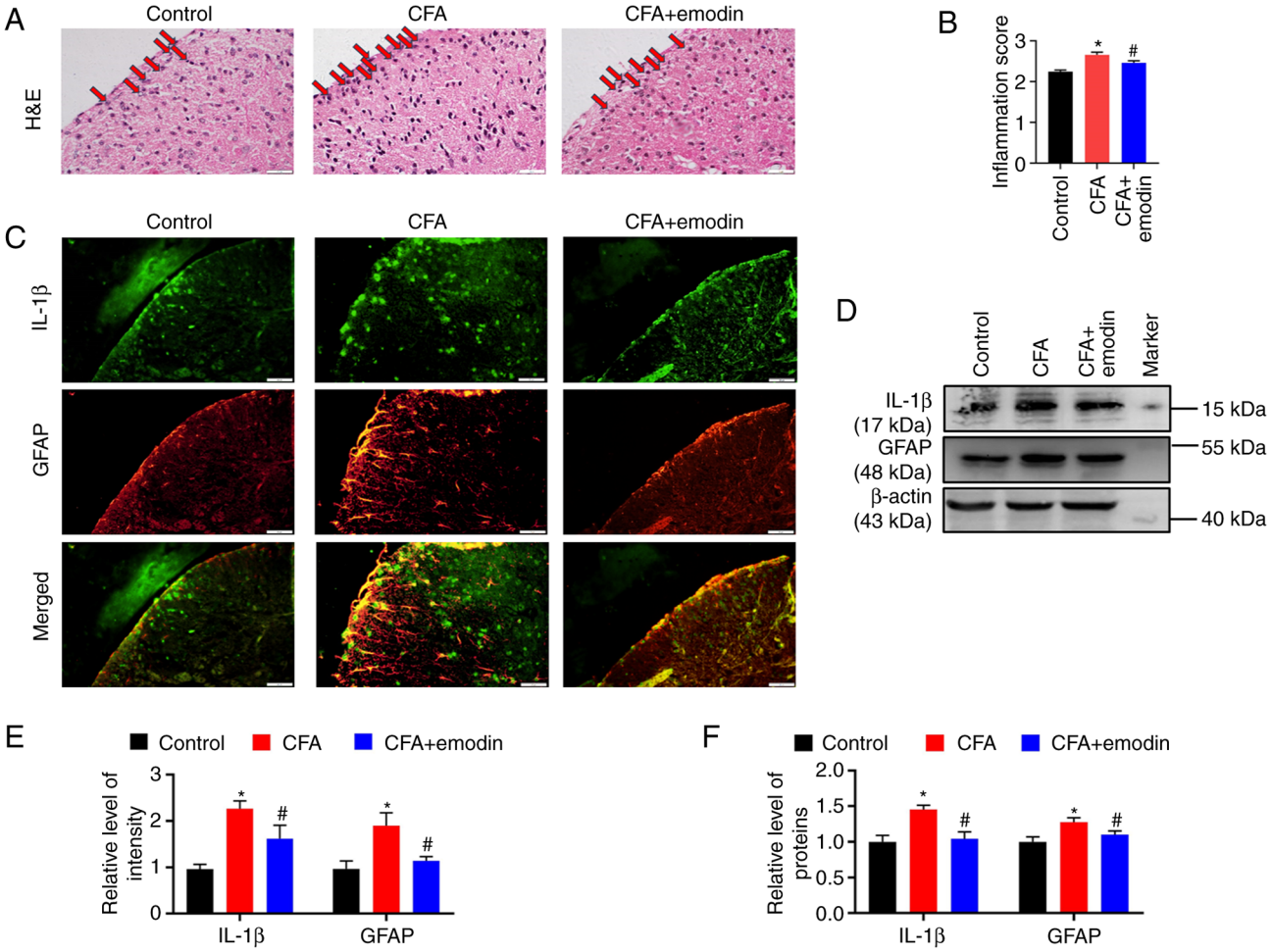

Figure 2. Emodin reduces spinal cord inflammatory response by inhibiting spinal cord astrocyte activation. Representative (A) hematoxylin and eosin-stained images and (B) inflammation score analysis of the spinal dorsal horn in each group. Scale bar, 20 μm. Representative (C) immunofluorescence staining images of IL-1β and GFAP and (E) quantitative fluorescence intensity analysis (overall magnification, x400; scale bar, 20 μm). (D) Western blot analysis and (F) quantification of the relative grey value of IL-1β and GFAP. Data are presented as the mean ± SD (n=5). *P<0.05 vs. control group; $^{\#}$P<0.05 vs. CFA group. GFAP, glial fibrillary acidic protein; CFA, complete Freund's adjuvant.

treatment also increased the latency to fall in CFA-induced mice, 354.27 ± 35.95, 367.16 ± 33.36 and 382.72 ± 32.39, on days 15 to 17, respectively (Fig. 1D). As a result, emodin alleviated pain behavior and improved motor ability in the CFA mice.

Emodin reduces spinal cord inflammatory response by inhibiting spinal cord astrocyte activation. For CFA mice, a significant inflammatory infiltration was found in the spinal dorsal horn with the inflammatory scores at 2.65 ± 0.06, whereas emodin treatment reduced the inflammatory infiltration to 2.45 ± 0.05 (Fig. 2A and B). Activated astrocytes are a major source of a number of pro-inflammatory cytokines and GFAP is used as a marker of abnormal proliferation and activation of astrocytes (22). The fluorescence intensities of IL-1β and GFAP in spinal dorsal horn of CFA group were enhanced, with the relative intensity at 2.26 ± 0.17 and 1.90 ± 0.28, respectively. The emodin treatment decreased the IL-1β and GFAP intensity to 1.62 ± 0.29 and 1.14 ± 0.09, respectively (Fig. 2C and E). As revealed by western blotting, the CFA group had higher spinal expression levels of IL-1β and GFAP than the control group, with the relative grey values of 1.45 ± 0.06 and 1.28 ± 0.06, respectively. The levels of IL-1β and GFAP were reduced to 1.04 ± 0.10 and 1.10 ± 0.05, respectively (Fig. 2D and F) by emodin treatment.

Emodin decreases the activity of spinal NLPR3 inflammasome. IL-1β maturation is promoted by NLRP3 inflammasome activation (23). The fluorescence intensities of NLRP3 and caspase-1 in spinal dorsal horn of CFA group were enhanced, with the relative intensity at 1.60 ± 0.11 and 1.33 ± 0.08, respectively. The emodin treatment decreased the NLRP3 and caspase-1 intensity to 1.28 ± 0.13 and 1.13 ± 0.07, respectively (Fig. 3A-D). As revealed by western blotting, the CFA group had higher spinal expression levels of NLRP3 and cleaved caspase-1 than control group, with the relative grey values of 1.40 ± 0.11 and 2.35 ± 0.16, respectively. The levels of NLRP3 and cleaved caspase-1 were reduced to 0.97 ± 0.10 and 2.03 ± 0.15, respectively (Fig. 3E and F) by emodin administration.

Emodin prevents spinal HDAC6 activity. The ligand emodin and the X-ray crystal structures of HDAC6 were used in a molecular docking test (Fig. 4A-C). According to Auto Dock data, four electrovalent bonds are produced by emodin and

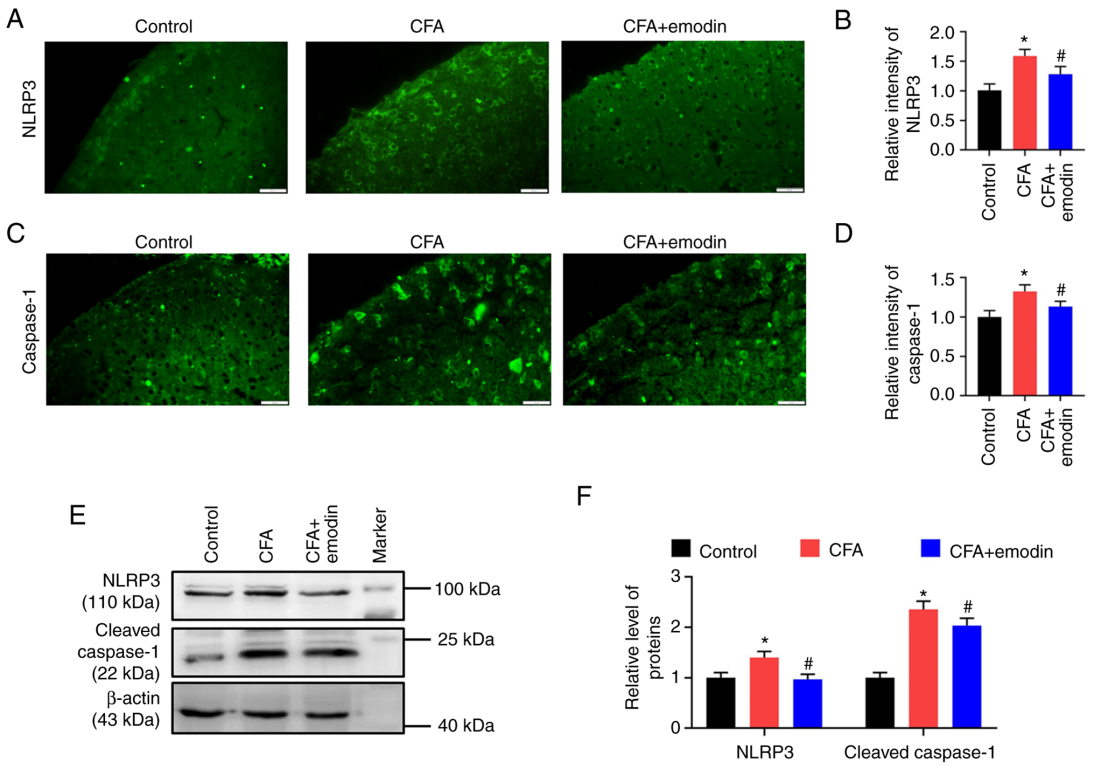

Figure 3. Changes in NLRP3 inflammasome components upon emodin treatment. (A-D) Representative immunofluorescence staining images and quantitative analysis of spinal NLRP3 and caspase-1 in the control, CFA and CFA + emodin groups. Scale bar, 20 μm. (E) Representative western blots and (F) quantitation examination of NLRP3 and cleaved caspase-1 expression levels the in spinal cords of the control, CFA and CFA + emodin groups. Data are presented as the mean ± SD (n=5). *P<0.05 vs. control group, $^{\#}$P<0.05 vs. CFA group. NLRP3, Nod-like receptor family pyrin domain-containing 3; CFA, complete Freund's adjuvant.

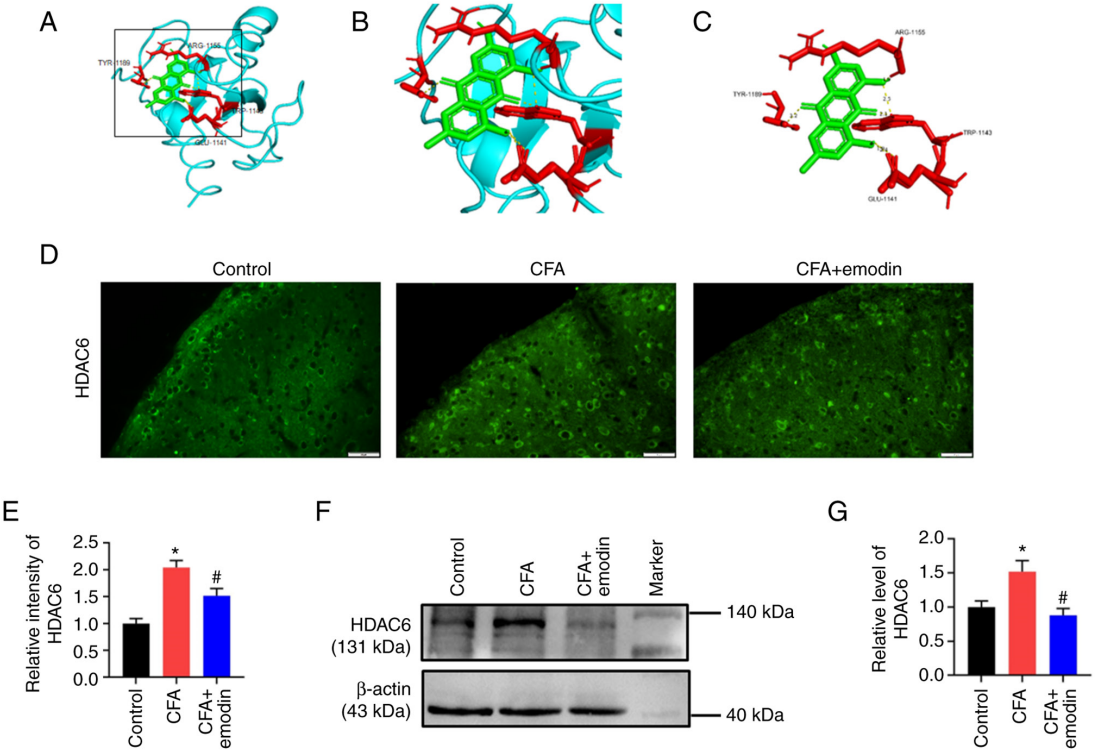

Figure 4. Effect of emodin treatment on HDAC6 activity. (A) The modeled 3D structure of HDAC6 docked with emodin. (B) An enlarged view of the binding site is displayed in the inset box. (C) The interaction bonds of HDAC6 with emodin. The HDAC6 protein is shown in cyan, emodin is colored green, the interacting residues as red, bonds are shown as yellow dotted lines and bond lengths are depicted as numbers. (D) Representative immunofluorescence staining images and (E) quantitative intensity analysis of HDAC6 of each group. Scale bar, 20 μm. Representative (F) western blots and (G) quantitation of HDAC6 expression levels. Data are presented as the mean ± SD (n=5). *P<0.05 vs. control group, $^{\#}$P<0.05 vs. CFA group. HDAC6, histone deacetylase 6; CFA, complete Freund's adjuvant.

HDAC6 at residues ARG-1155, TYR-1189, GLU-1141 and TRP-1143. The electrovalent bond distances were 1.9, 3.2, 2.4 and 2.1 Å between HDAC6 and emodin, while the binding affinity was -8.7 kcal/mol. The increased HDAC6 fluorescence intensity in the spinal dorsal horn was observed in the CFA group, with a relative intensity of 2.04 ± 0.13. HDAC6 intensity was decreased to 1.52 ± 0.13 upon emodin treatment (Fig. 4D and E). The spinal HDAC6 protein level of CFA group was higher than the control group; the relative grey value was 1.52 ± 0.16. HDAC6 protein level was downregulated by emodin treatment to 0.88 ± 0.10 (Fig. 4F and G).

Discussion

The present study discovered that emodin reduced CFA-induced pain by controlling HDAC6. HDAC6 works as a therapeutic target for chronic pain (24). HDAC6 inhibitor SW-100 treatment restores deacetylation of α-tubulin in sciatic nerve and alleviates mechanical allodynia and hyperalgesia in the peripheral neuropathy mouse model (25). Chemotherapy-induced peripheral neuropathy model mice treated with HDAC6 inhibitor recover from mechanical allodynia and spontaneous pain caused by cisplatin (26). HDAC6 genetic deletion prevents the mechanical allodynia that cisplatin causes (27). The present study found increased spinal HDAC6 expression in CFA-induced inflammatory pain model mice. Emodin binds with HDAC6 at a high binding affinity, producing a comparatively stable docking outcome (28). In the meantime, in the cardiac hypertrophy model, emodin inhibits HDAC activity and increases histone acetylation, while blocking pathological cardiac hypertrophy (29). Hence, it was hypothesized that emodin binds with HDAC6 and inhibits its activity.

Emodin suppresses spinal inflammation by regulating HDAC6. It is reported that HDAC6 serves as a dynein adaptor for the purpose of facilitating transport and assembling NLRP3 inflammasome (30). HDAC6 inhibition decreases the NLRP3 and IL-1β levels and suppresses nicotine-induced pyroptosis in atherosclerosis model mice (31). In LPS-induced mice, HDAC6 degrader application lessened activation of NLRP3 inflammasome (32). In a Parkinson's disease mouse model, the pharmacological suppression of HDAC6 by tubastatin A reduces NLRP3 expression and the maturation of IL-1β (33). The present study suggested that emodin treatment disrupted the binding of HDAC6 and NLRP3 and suppressed NLRP3 inflammasome activation. Furthermore, HDAC6 participates in pro-inflammatory interleukin expression through NF-κB signaling, which induces the pro-IL-1β and NLRP3 transcription expression (34). In arthritis model animals, HDAC6 depletion post-transcriptionally upregulates NF-κB inhibitor and downregulates NF-κB reporter activation and prevents the nuclear translocation of NF-κB subunits (35). HDAC6 mediates deacetylation of NF-κB and plays an inhibitory effect on invasion (36). The present study indicated that emodin administration reduced NF-κB-mediated neuroinflammation in chronic pain.

During chronic pain processing, NLRP3 inflammasome is activated and spinal inflammation is triggered. Emodin treatment binds HDAC6, weakens the HDAC6-NLRP3 interaction, reduces NLRP3 inflammasome reaction and suppresses spinal inflammation while alleviating chronic inflammatory pain.

Acknowledgements

Not applicable.

Funding

The present study was funded by the Hubei University of Science and Technology Program (grant nos. BK202213, 2021WG06, 2022YKY02 and 2022YKY09), as well as the Research Project of the Hubei Provincial Department of Education (grant nos. ZY2023F109, B2022186 and B2022185).

Availability of data and materials

The datasets used and/or analyzed during the current study are available from the corresponding author on reasonable request.

Authors' contributions

Each author significantly contributed to the present study. MX and FZ conceived and designed the study. The experiments were conducted by DC, YX and TC. SZ, WM and HZ gathered and analyzed the data. The manuscript was drafted and edited by MX and FZ. The final manuscript was reviewed and approved by all authors. DC, YX and TC confirm the authenticity of all the raw data. All authors read and approved the final manuscript.

Ethics approval and consent to participate

The Hubei University of Science and Technology Ethics Committee approved the present study (approval number 2020-01-900). All experiments were performed in accordance with international and local guidelines on the ethical use of animals.

Patient consent for publication

Not applicable.

Competing interests

The authors declare that they have no competing interests.

References

1. Mills SEE, Nicolson KP and Smith BH: Chronic pain: A review of its epidemiology and associated factors in population-based studies. Br J Anaesth 123: e273-e283, 2019.
2. Cohen SP, Vase L and Hooten WM: Chronic pain: An update on burden, best practices, and new advances. Lancet 397: 2082-2097, 2021.
3. Tobin DG, Lockwood MB, Kimmel PL, Dember LM, Eneanya ND, Jhamb M, Nolin TD, Becker WC, Fischer MJ and HOPE Consortium (Corporate Author): Opioids for chronic pain management in patients with dialysis-dependent kidney failure. Nat Rev Nephrol 18: 113-128, 2022.
4. Santoni A, Santoni M and Arcuri E: Chronic cancer pain: Opioids within tumor microenvironment affect neuroinflammation, tumor and pain evolution. Cancers (Basel) 14: 2253, 2022.
5. Dong ZB, Wang YJ, Wan WJ, Wu J, Wang BJ, Zhu HL, Xie M and Liu L: Resveratrol ameliorates oxaliplatin-induced neuropathic pain via anti-inflammatory effects in rats. Exp Ther Med 24: 586, 2022.

6. Ji RR, Nackley A, Huh Y, Terrando N and Maixner W: Neuroinflammation and central sensitization in chronic and widespread pain. Anesthesiology 129: 343-366, 2018.
7. Linnerbauer M, Wheeler MA and Quintana FJ: Astrocyte crosstalk in CNS inflammation. Neuron 108: 608-622, 2020.
8. Huang Y, Xu W and Zhou R: NLRP3 inflammasome activation and cell death. Cell Mol Immunol 18: 2114-2127, 2021.
9. Zhang YZ, Zhang YL, Huang Q, Huang C, Jiang ZL, Cai F and Shen JF: AdipoRon alleviates free fatty acid-induced myocardial cell injury via suppressing Nlrp3 inflammasome activation. Diabetes Metab Syndr Obes 12: 2165-2179, 2019.
10. Choudhury SM, Ma X, Zeng Z, Luo Z, Li Y, Nian X, Ma Y, Shi Z, Song R, Zhu Z, *et al*: Senecavirus a 3D interacts with NLRP3 to induce IL-1β production by activating NF-κB and ion channel signals. Microbiol Spectr 10: e0209721, 2022.
11. Chen R, Yin C, Fang J and Liu B: The NLRP3 inflammasome: An emerging therapeutic target for chronic pain. J Neuroinflammation 18: 84, 2021.
12. Yu S, Zhao G, Han F, Liang W, Jiao Y, Li Z and Li L: Muscone relieves inflammatory pain by inhibiting microglial activation-mediated inflammatory response via abrogation of the NOX4/JAK2-STAT3 pathway and NLRP3 inflammasome. Int Immunopharmacol 82: 106355, 2020.
13. Khan N, Kuo A, Brockman DA, Cooper MA and Smith MT: Pharmacological inhibition of the NLRP3 inflammasome as a potential target for multiple sclerosis induced central neuropathic pain. Inflammopharmacology 26: 77-86, 2018.
14. Dong X, Fu J, Yin X, Cao S, Li X, Lin L, Huyiligeqi and Ni J: Emodin: A review of its pharmacology, toxicity and pharmacokinetics. Phytother Res 30: 1207-1218, 2016.
15. Zhang X, Li J and Guan L: Emodin reduces inflammatory and nociceptive responses in different pain-and inflammation-induced mouse models. Comb Chem High Throughput Screen 26: 989-1000, 2023.
16. Gao Y, Liu H, Deng L, Zhu G, Xu C, Li G, Liu S, Xie J, Liu J, Kong F, *et al*: Effect of emodin on neuropathic pain transmission mediated by P2X2/3 receptor of primary sensory neurons. Brain Res Bull 84: 406-413, 2011.
17. Sun T, Wang J, Li X, Li YJ, Feng D, Shi WL, Zhao MG, Wang JB and Wu YM: Gastrodin relieved complete Freund's adjuvant-induced spontaneous pain by inhibiting inflammatory response. Int Immunopharmacol 41: 66-73, 2016.
18. Hao M, Tang Q, Wang B, Li Y, Ding J, Li M, Xie M and Zhu H: Resveratrol suppresses bone cancer pain in rats by attenuating inflammatory responses through the AMPK/Drp1 signaling. Acta Biochim Biophys Sin (Shanghai) 52: 231-240, 2020.
19. Mao Y, Wang C, Tian X, Huang Y, Zhang Y, Wu H, Yang S, Xu K, Liu Y, Zhang W, *et al*: Endoplasmic reticulum stress contributes to nociception via neuroinflammation in a murine bone cancer pain model. Anesthesiology 132: 357-372, 2020.
20. Shi X, Bai H, Wang J, Wang J, Huang L, He M, Zheng X, Duan Z, Chen D, Zhang J, *et al*: Behavioral assessment of sensory, motor, emotion, and cognition in rodent models of intracerebral hemorrhage. Front Neurol 12: 667511, 2021.
21. Seeliger D and de Groot BL: Ligand docking and binding site analysis with PyMOL and Autodock/Vina. J Comput Aided Mol Des 24: 417-422, 2010.
22. Zhang D, Hu X, Qian L, O'Callaghan JP and Hong JS: Astrogliosis in CNS pathologies: Is there a role for microglia? Mol Neurobiol 41: 232-241, 2010.
23. Cao DY, Zhang ZH, Li RZ, Shi XK, Xi RY, Zhang GL, Li F and Wang F: A small molecule inhibitor of caspase-1 inhibits NLRP3 inflammasome activation and pyroptosis to alleviate gouty inflammation. Immunol Lett 244: 28-39, 2022.
24. Prior R, Van Helleputte L, Klingl YE and Van Den Bosch L: HDAC6 as a potential therapeutic target for peripheral nerve disorders. Expert Opin Ther Targets 22: 993-1007, 2018.
25. Picci C, Wong VSC, Costa CJ, McKinnon MC, Goldberg DC, Swift M, Alam NM, Prusky GT, Shen S, Kozikowski AP, *et al*: HDAC6 inhibition promotes alpha-tubulin acetylation and ameliorates CMT2A peripheral neuropathy in mice. Exp Neurol 328: 113281, 2020.
26. Krukowski K, Ma J, Golonzhka O, Laumet GO, Gutti T, van Duzer JH, Mazitschek R, Jarpe MB, Heijnen CJ and Kavelaars A: HDAC6 inhibition effectively reverses chemotherapy-induced peripheral neuropathy. Pain 158: 1126-1137, 2017.
27. Ma J, Trinh RT, Mahant ID, Peng B, Matthias P, Heijnen CJ and Kavelaars A: Cell-specific role of histone deacetylase 6 in chemotherapy-induced mechanical allodynia and loss of intraepidermal nerve fibers. Pain 160: 2877-2890, 2019.
28. Zhou P, Zhou R, Min Y, An LP, Wang F and Du QY: Network pharmacology and molecular docking analysis on pharmacological mechanisms of astragalus membranaceus in the treatment of gastric ulcer. Evid Based Complement Alternat Med 2022: 9007396, 2022.
29. Evans LW, Bender A, Burnett L, Godoy L, Shen Y, Staten D, Zhou T, Angermann JE and Ferguson BS: Emodin and emodin-rich rhubarb inhibits histone deacetylase (HDAC) activity and cardiac myocyte hypertrophy. J Nutr Biochem 79: 108339, 2020.
30. Magupalli VG, Negro R, Tian Y, Hauenstein AV, Di Caprio G, Skillern W, Deng Q, Orning P, Alam HB, Maliga Z, *et al*: HDAC6 mediates an aggresome-like mechanism for NLRP3 and pyrin inflammasome activation. Science 369: eaas8995, 2020.
31. Xu S, Chen H, Ni H and Dai Q: Targeting HDAC6 attenuates nicotine-induced macrophage pyroptosis via NF-κB/NLRP3 pathway. Atherosclerosis 317: 1-9, 2021.
32. Cao Z, Gu Z, Lin S, Chen D, Wang J, Zhao Y, Li Y, Liu T, Li Y, Wang Y, *et al*: attenuation of NLRP3 inflammasome activation by indirubin-derived PROTAC targeting HDAC6. ACS Chem Biol 16: 2746-2751, 2021.
33. Yan S, Wei X, Jian W, Qin Y, Liu J, Zhu S, Jiang F, Lou H and Zhang B: Pharmacological inhibition of HDAC6 attenuates NLRP3 inflammatory response and protects dopaminergic neurons in experimental models of parkinson's disease. Front Aging Neurosci 12: 78, 2020.
34. He J, Zhou Y, Xing J, Wang Q, Zhu H, Zhu Y and Zou MH: Liver kinase B1 is required for thromboxane receptor-dependent nuclear factor-κB activation and inflammatory responses. Arterioscler Thromb Vasc Biol 33: 1297-1305, 2013.
35. Barter MJ, Butcher A, Wang H, Tsompani D, Galler M, Rumsby EL, Culley KL, Clark IM and Young DA: HDAC6 regulates NF-κB signalling to control chondrocyte IL-1-induced MMP and inflammatory gene expression. Sci Rep 12: 6640, 2022.
36. Yang CJ, Liu YP, Dai HY, Shiue YL, Tsai CJ, Huang MS and Yeh YT: Nuclear HDAC6 inhibits invasion by suppressing NF-κB/MMP2 and is inversely correlated with metastasis of non-small cell lung cancer. Oncotarget 6: 30263-30276, 2015.